JVSTA Journal of Vacuum Science & Technology A

In situ formation and electron-spectroscopic study of bis(arene) V and Cr compounds on a graphite surface

Victor M. Bermudez

Citation: Journal of Vacuum Science & Technology A **31**, 031402 (2013); doi: 10.1116/1.4794194
View online: http://dx.doi.org/10.1116/1.4794194
View Table of Contents: http://scitation.aip.org/content/avs/journal/jvsta/31/3?ver=pdfcov
Published by the AVS: Science & Technology of Materials, Interfaces, and Processing

In situ formation and electron-spectroscopic study of bis(arene) V and Cr compounds on a graphite surface

Victor M. Bermudez[a)]
Electronics Science and Technology Division, Naval Research Laboratory, Washington, DC 20375-5347

(Received 27 January 2013; accepted 19 February 2013; published 7 March 2013)

Thin layers of bis(arene) transition metal (TM) compounds have been formed *in situ* in ultra-high vacuum by depositing Cr or V metal on top of a film of benzene (Bz) or toluene (Tol) ice at 100 K on a graphite substrate. The species thus formed are $Cr(C_6H_6)_2$, $V(C_6H_6)_2$, or $Cr(C_6H_5\text{-}CH_3)_2$ (termed $CrBz_2$, VBz_2, or $Cr(Tol)_2$), and the valence structures have been examined using electron energy loss and ultraviolet photoemission spectroscopies (ELS and UPS). The reaction is "clean" in that there is no indication of side reactions or unwanted by-products, although a small coverage of unreacted TM atoms appears unavoidable. A simple ring substituent (CH_3) remains intact during the reaction. Thus, it should be possible to synthesize and study species that are not readily available (or cannot easily be made) in bulk form or that have too low vapor pressure to allow easy *in situ* deposition. Data have been obtained for VBz_2 and $Cr(Tol)_2$, the valence structures of which have not previously been studied in detail using UPS and ELS. Although deeper-lying arene orbitals are essentially unperturbed by formation of the bis(arene)TM sandwich, subtle differences in the TM-related orbitals have been observed and discussed in comparison to $CrBz_2$ with the aid of density functional theory. In the case of VBz_2, clear evidence is seen for a molecular reorientation during annealing, based on the ELS polarization dependence. Electron transfer between an adsorbed bis(arene)TM and graphite depends on the occupancy of the highest occupied molecular orbital (HOMO) and on its energy relative to the Fermi level (E_F). The small amount of unreacted TM resulting from *in situ* synthesis causes a large decrease in work function, which shifts the adsorbate HOMO to below E_F and thus impedes electron transfer to highly oriented pyrolytic graphite. This is an obstacle to forming doping layers by this method.
[http://dx.doi.org/10.1116/1.4794194]

I. INTRODUCTION

The doping of semiconducting single-wall carbon nanotubes (SWCNTs) and graphene is a subject of significant importance since it enables the modification of electronic properties and, thus, the engineering of carbon nanostructures for specific applications. There has been extensive theoretical and experimental effort in this field, some of which is reviewed elsewhere.[1–3] The term "doping" as used here includes manipulation of the band gap as well as the more traditional concept of modifying the free-carrier concentration. One very promising approach involves incorporating a transition metal (TM) or a TM compound by some means, either on the surface or by encapsulation within an SWCNT. An advantage of this approach is that an appropriately chosen TM structure will be stable against oxidation, whereas a bare TM atom is generally not. Another expected benefit[4–6] is that the π-bonded network of the graphene or SWCNT remains intact, so that carrier mobility should not be significantly degraded. This contrasts with other methods in which sp^3-hybridized C atoms form at dopant bonding sites.

One particularly stable class of TM compounds[7] is the bis(arene)TM "sandwich" in which a TM atom is bonded between two π-bonded organic rings, or arenes. An archetypal example is bis(benzene)Cr [$Cr(\eta^6\text{-}C_6H_6)_2$, Fig. 1] where η^6 indicates that the Cr is coordinated to all six C atoms in the benzene (Bz) ring, and theoretical studies have examined analogs of the bis(arene)TM sandwich in which one side is graphene[4–6] and the other is an arene, typically Bz. A variant of this approach that has to some extent been demonstrated experimentally is to use a bis(arene)TM itself as the dopant. Ferrocene ($Fe(\eta^5\text{-}C_5H_5)_2$ or $FeCp_2$, where Cp ≡ cyclopentadiene) can be encapsulated into SWCNTs from solution[8] or from the vapor,[9,10] although the resulting electronic properties have not been characterized. Theory indicates *n*-type doping for cobaltocene ($Co(\eta^5\text{-}C_5H_5)_2$ or $CoCp_2$) encapsulated in an SWCNT[11,12] or adsorbed on graphene.[13] This has been verified experimentally[14] for $CoCp_2$ on highly oriented pyrolytic graphite (HOPG), which shows evidence for electron transfer from the adsorbate to the substrate.

Doping by means of a bis(arene)TM is closely related to the electronic structure of such species. The free Cr atom has the electronic configuration $(Ar)3d^54s^1$, and the metal–ligand bonding in $CrBz_2$ has been analyzed quantitatively[15] in terms of specific orbital interactions. The Cr $3d_z^2$ orbital transforms as the a_{1g} representation of the D_{6h} point group describing $CrBz_2$ in the eclipsed structure (cf. Fig. 1). The $3d_z^2$ is a nonbonding orbital (NBO) and is the highest occupied molecular orbital (HOMO). The $3d_{x^2-y^2}$ and $3d_{xy}$ orbitals (HOMO-1) belong to e_{2g} and are strongly δ-bonding, while the Cr $3d_{xz}$ and $3d_{yz}$ orbitals (HOMO-2) transform as e_{1g} and are weakly π-bonding. The resulting system has a very stable 18-electron "Kr-like" valence structure (six electrons from Cr and six from each of the rings), which gives a $^1A_{1g}$ ground state.

a)Electronic mail: victor.bermudez@nrl.navy.mil

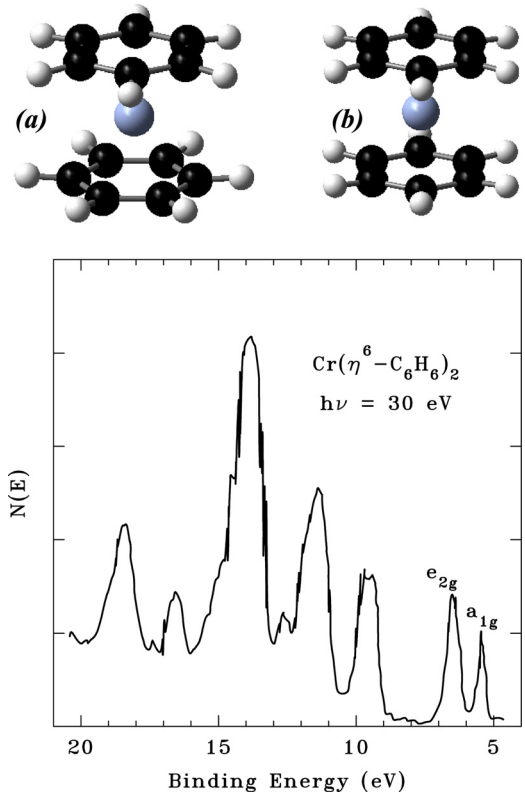

FIG. 1. (Color online) (a) Staggered and (b) eclipsed Cr(η^6-C_6H_6)$_2$; (c) experimental UPS data for Cr(η^6-C_6H_6)$_2$ vapor (hν = 30 eV) from Ref. 16 (with permission). The binding energy reference is the vacuum level. The very sharp features are artifacts incurred during digitization of the published spectrum.

Figure 1 shows gas-phase ultraviolet photoemission spectroscopy (UPS) data,[16] which are very similar to those for a condensed multilayer.[17] The distinguishing characteristic of Cr–C_6H_6 bonding is the appearance of the a_{1g} and e_{2g} features, while deeper-lying structure is similar to that of molecular benzene.[17] V(η^6-C_6H_6)$_2$ (or VBz_2) also forms an eclipsed structure but is a 17-electron system with a single unpaired electron in the a_{1g} NBO, which gives a $^2A_{1g}$ ground state.

For a given TM the NBO can act as a donor or acceptor level depending on occupancy and on the energy separation from the SWCNT or graphene band edges, as has been shown theoretically[11–13] for $CoCp_2$. Cobaltocene has a 19-electron valence structure (9 from Co and 10 from the two rings), and the singly occupied NBO on the Co lies above the conduction band minimum (CBM) in the vicinity of the SWCNT Γ-point. Encapsulated $CrBz_2$ shows,[12] for an SWCNT of an appropriate diameter, the NBO lying <0.1 eV below the CBM near the Γ-point, making it potentially active as a shallow donor. Other theoretical work[18] has shown that adsorption of $FeCp_2$ and of ruthenocene, the Ru analog of $FeCp_2$, can modify the electronic properties of graphene that has been doped with foreign atoms such a B or N. Further advances might be achieved by investigating other potential bis(arene)TM species as graphene dopants beyond $CoCp_2$, which to date is the only such species to have been experimentally demonstrated[14] for this application. Actually forming such systems, however, raises certain practical issues related to the synthesis and deposition of bis(arene)TMs, which are addressed here.

The purpose of the present work is to examine the feasibility of a novel approach to doping via adsorption of bis(arene)TMs, using $CrBz_2$ and VBz_2 as representative compounds and HOPG as a simulant for graphene. Since the valence electronic structure is of most interest, this work uses UPS and electron energy loss spectroscopy (ELS) performed in ultra-high vacuum (UHV). Such data are necessary for comparison with the theoretical results cited above. Forming a sample *in situ* under UHV conditions[17] raises the issue of the low vapor pressures of bis(arene)TMs (e.g., 4.56×10^{-4} Torr for $CrBz_2$ at 50 °C, Ref. 19). This will be circumvented using a method, first reported by Sklarek *et al.*,[20] in which the metal of interest is vapor-deposited onto a layer of solid arene ice. This technique is conceptually similar to metal-vapor synthesis[21] (or co-condensation), in which vapors of the metal and the organic reagent are condensed together on a substrate. However, the process described by Sklarek *et al.*[20] is more compatible with an UHV environment since only a small arene dose is needed to form the required ice layer. This was demonstrated for the *in situ* synthesis of $CrBz_2$ but to our knowledge has not been reported for other TMs or arenes. In addition to overcoming the problem of low organometallic vapor pressure, this allows the easy synthesis of thin layers of bis(arene)TMs that are not available (or cannot be made) in bulk form. Thus, quite apart from any interest in doping, *in situ* spectroscopic studies can be performed on species not readily obtainable by conventional means.

II. METHODS

A. Experiment

All experiments were done in a standard stainless-steel UHV chamber with a base pressure of $\sim 7 \times 10^{-11}$ Torr. The electron spectrometer was a double-pass cylindrical mirror analyzer (CMA) which, for UPS, was operated in the "retard" (constant-resolution) mode with electron-counting detection. The excitation source was the HeII (hν = 40.81 eV) line of a differentially pumped dc discharge in He gas, and the CMA pass energy was 25 eV, giving a total instrumental resolution of ~0.40 eV. Binding energies (BEs) were referenced to the Fermi edge of metallic clusters[22,23] formed on HOPG at room temperature and also to the HOPG slow-secondary peak.[24] The sample work function (φ_S) was measured using the kinetic energy threshold for secondary-electron emission with a small negative bias applied to the sample and the CMA resolution increased to ~0.16 eV. The threshold was obtained by a linear extrapolation of the low-energy edge to zero counts. The work function of clean, undamaged HOPG thus obtained was $\varphi_S = 4.6 \pm 0.1$ eV at 100 K, which is in reasonable agreement with a previous result[14] of 4.4 eV.

For ELS, data were obtained with an $E_p = 90$ eV, $i_p \approx 0.3\ \mu A/cm^2$ electron beam from the coaxial gun of the CMA. The current density was kept low to avoid damage to the organic species, the absence of which was verified by repeated scans of the same area of the surface. The resolution, given by the full-width at half-maximum (FWHM) of the

elastic peak, was 0.5 eV, and data were recorded as N(E) vs E using electron counting. Auger electron spectroscopy (AES) data were obtained in the form of d(E·N(E))/dE in the nonretard, first-derivative mode using a 3 keV, ~4 μA primary beam with a 2 eV peak-to-peak modulation. In all experiments, the sample normal made an angle of 25° with the CMA axis.

A sample of HOPG was mounted on a variable-temperature stage and cleaned *in situ* by annealing at 1200 K, which has been shown[25] to yield a high-quality surface. The sample temperature was measured using an optical pyrometer, and following this treatment no impurities were detected in AES. Cr was deposited *in situ* using a resistively heated Cr-plated W wire,[26] and V was deposited from a resistively heated ribbon (99.8% purity) which had been etched briefly in 1:1 HNO_3:H_2O prior to mounting to remove any gross surface contamination. The chamber pressure remained below 2×10^{-9} Torr during metal deposition, and residual gas analysis showed that H_2 was the main component in the UHV ambient during deposition. Metal deposition was controlled using a quartz crystal oscillator thickness monitor, and the actual coverages were determined using AES (see the supplementary material[27]). The purity of the metal layers was evaluated after deposition at ~100 K on bare HOPG (i.e., with no arene ice layer). The O KLL spectrum overlaps the V and Cr LMM spectra but, in the case of Cr, is sufficiently separated[28] that O contamination can be detected directly. For V, the main O KLL feature, at ~510 eV, overlaps the V peak near 511 eV.[29] Hence, O was detected on V by observing the relative peak-to-peak heights of the V transitions at 511 and 475 eV, which is 0.25 for clean V at $E_p = 3$ keV.[29] No O was detectable in the freshly deposited metal layers.

Exposure to reagent vapor was done using a calibrated-pinhole molecular-beam doser.[30] The reagent-grade liquids were previously degassed by repeated freeze-pump-thaw cycles with freezing being done in dry ice (Bz) or liquid N_2 [toluene (Tol)]. The nude ionization gauge was switched off before dosing in order to avoid excitation of molecular species. The sample temperature was measured using a chromel/alumel thermocouple attached to the cooled Cu block in thermal contact with the sample. The temperature reading was checked by noting the point at which condensed Bz disappeared in ELS and UPS experiments. This occurred within 10 K of the reported[31] desorption temperature (152 K) for a Bz monolayer (ML) on HOPG.

After each series of experiments, the Cr was thermally desorbed at 1200 K to re-clean the surface. This removed all but a small residue, ~0.05 ML, which is thought to represent Cr retained in fissures in the HOPG surface or strongly adsorbed at defects. Here, one ML means one Cr per surface C atom (i.e., 3.83×10^{15} atoms/cm^2). In the case of V, metallic deposits could not be completely removed by heating in UHV to 1300 K, the highest temperature attainable with the present apparatus. Formation of V carbide might occur at this temperature, but the coverage was not sufficiently high that a distinct change in the C KLL line shape[32] could be seen. V was removed using 1 keV Ar^+-ion bombardment at room temperature (at a total dose of ~10 Ar^+ per surface C) followed by annealing at 1200 K. It should be noted that the Cr experiments were all performed on HOPG that had never been ion bombarded.

B. Computation

Density functional theory (DFT) calculations for free molecules were done, mainly for the purpose of obtaining model UPS spectra, using the *Gaussian 09* program suite.[33] The TPSS functional was used since it has been shown[34] to give good structural and bond-energy results for $CrBz_2$ and related species. For C and H, 6–311 G(d,p) basis sets were used, and larger basis sets (6–311$^+$G(2d,2p)) gave no significant difference in the optimized geometries. Some calculations were also done for anions, and for these 6–311^{++}G(d,p) basis sets were used for C and H since diffuse functions are generally required in this case. For TMs, the Stuttgart-Dresden relativistic effective-core pseudopotentials (ECPs) of Dolg *et al.*[35] were used since these have been shown[36] to give good results for $CrBz_2$. These are small-core ECPs that replace only the metal 1s, 2s, and 2p shells. Spin-unrestricted calculations were done for species having an unpaired electron, and all results were checked for wavefunction instabilities[37] and for imaginary vibrational frequencies. "Tight" convergence criteria and an "ultra-fine" integration grid were used in all calculations.

Model UPS spectra were computed using the one-electron energies of the occupied orbitals. A Gaussian of unit area was placed at each energy and the sum of all such peaks obtained. Thus, all orbitals are assumed to have the same photoionization cross section. A Gaussian FWHM of 1.0 eV was chosen so that the computed line widths approximated those in the experiment. This includes the purely instrumental broadening of 0.40 eV plus additional contributions from "solid-state effects" (intermolecular interaction and disorder in the condensed layers).

III. RESULTS

A. Energy loss spectroscopy

The ELS data [Figs. 2(a) and 2(b)] for bare HOPG and for solid Bz in the range of valence and π plasmon excitation show, respectively, a π plasmon[38] at ~6.5 eV and a $\pi \rightarrow \pi^*$ excitation[39] at 7.0 eV. The Bz spectrum shows an additional weak feature at 10 eV that has been associated[40] with the extent of crystallinity. Sklarek *et al.*[20] have reported the *in situ* synthesis of $CrBz_2$ by deposition of Cr onto a layer of Bz ice and characterized the product using core-level x-ray photoemission spectroscopy. We have repeated this process, depositing ~0.20 ML of Cr on Bz ice at 100 K, and have studied the valence excitations of the resulting material using ELS and UPS. The ice thickness is estimated to be a few tens of MLs, based on the Bz dose and the assumption of unity sticking coefficient at 100 K. In this case, an ML refers to a close-packed layer of flat-lying Bz rings. When necessary, the sample was warmed to ~170 K to desorb unreacted Bz and then cooled back to 100 K for data collection. For thinner ice layers, this was not needed since most of the Bz either reacted with the metal or desorbed due to the energy released in the deposition. A recent study[41] of Ag, Mg, and Al deposited on Bz ice at 30 K reports a complex mix of reaction

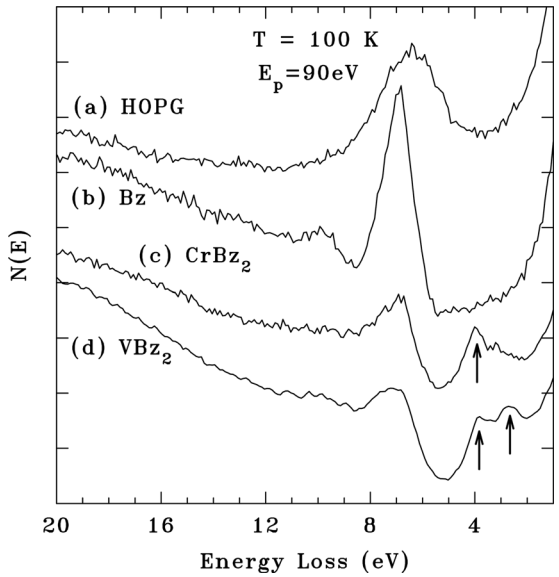

FIG. 2. ELS data at 100 K for (a) clean HOPG, (b) a thick layer of benzene ice, (c) after deposition of ~0.20 ML of Cr, and (d) after deposition of ~0.20 ML of V. The spectra have been scaled for equal intensity in the elastic peak and have been displaced vertically for clarity. The arrows mark some of the features discussed in the text.

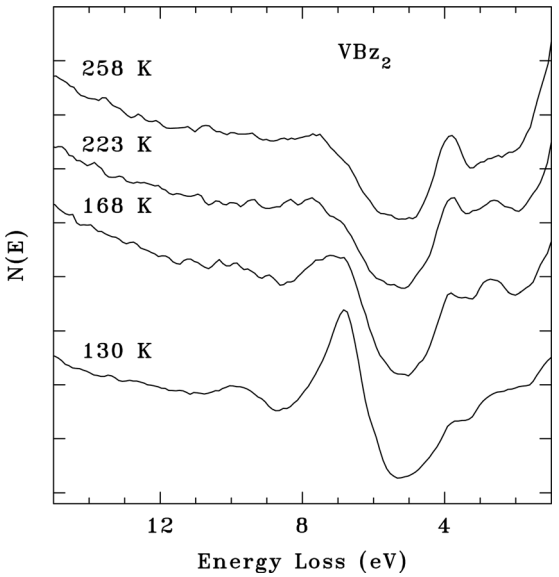

FIG. 3. ELS vs annealing for VBz_2. In each case, the sample is raised to the temperature indicated and then returned to 100 K for data collection. The 168 K spectrum is the same as that shown in Fig. 2(d). The spectra have been scaled for equal intensity in the elastic peak and have been displaced vertically for clarity.

products for Al but not for Ag or Mg. The controlling factor is thought to be the metal ionization potential (IP) which is low for Al (5.98 eV) but higher for Ag and Mg (7.57 and 7.64 eV, respectively). The IPs for V and Cr (6.74 and 6.76 eV, respectively[42]) are roughly midway between these values, and no indication of products other than VBz_2 and $CrBz_2$ was seen here or in Ref. 20.

With Cr added, a new feature is seen [Fig. 2(c)] at 4.0 eV. The absorption spectrum[43] of $CrBz_2$ vapor in the 2.7–5.3 eV range shows relatively narrow Rydberg transitions at 3.3 and 4.4 eV and a broad feature at ~4.0 eV, which is assigned to a valence excitation. If the initial state is the a_{1g} NBO, then the final state in the valence excitation would be either a_{2u} or e_{1u} under the electric-dipole selection rules for D_{6h} symmetry. A recent calculation[44] using time-dependent DFT places the $CrBz_2$ $a_{1g} \rightarrow a_{2u}$ transition at 3.3 eV, but the $a_{1g} \rightarrow e_{1u}$ energy was not given. VBz_2 was synthesized in the same manner as for $CrBz_2$, which suggests that this may be a general approach for the *in situ* synthesis of simple bis(arene)TMs. Data presented below will show that bis(toluene)Cr ($Cr(\eta^6\text{-}C_6H_5CH_3)_2$ or $Cr(Tol)_2$) can also be formed by this means. The VBz_2 ELS data [Fig. 2(d)] show a $\pi \rightarrow \pi^*$ transition at ~7.0 eV and two molecular excitations at ~2.6 and 3.8 eV, both of which have been assigned[43] to transitions originating from the e_{2g} (HOMO-1) orbital. Another study[45] assigns the 2.6 eV peak to an excitation of the a_{1g} (HOMO) orbital and also reports the onset of a strong, broad absorption at 6.2 eV in agreement with Fig. 2(d).

Figure 3 shows ELS data for VBz_2 as a function of annealing for a sample formed at 100 K. In all cases, the temperature was raised to the indicated value and then returned to 100 K for data collection. After the first anneal, at 130 K, the spectrum is still dominated by unreacted Bz; however, upon further annealing the relative intensity of the 2.6 and 3.8 eV losses is seen to be temperature dependent. The $\pi \rightarrow \pi^*$ transition also shows a loss of intensity and a ~0.5 eV shift to higher energy which may represent the loss of a contribution from unreacted Bz above 168 K. There appears to be little or no similar temperature dependence in the $CrBz_2$ ELS (not shown).

The effect of annealing on the 2.6 and 3.8 eV losses can be understood in terms of a molecular reorientation. Rubloff has shown[46] that, in the case of dipolar scattering, a polarization selection rule can be formulated for ELS whereby the intensity due to excitation of an adsorbate dipole parallel to the surface is reduced in magnitude by a factor of $(\varepsilon_1^2 + \varepsilon_2^2)$ relative to one that is normal to the surface. Here, ε_1 and ε_2 are the real and imaginary dielectric constants of the substrate at an energy equal to that of the transition being excited. Using the optical constants[47] for HOPG at 3 eV for polarization parallel to the surface gives a reduction factor of ~70; hence, only an excitation polarized perpendicular to the surface can be detected for purely dipolar scattering.

Both assignments[43,45] of the VBz_2 optical spectrum agree that the 3.8 eV transition is $e_{2g} \rightarrow e_{2u}$. In the molecular D_{6h} point group, $e_{2g} \otimes e_{2u} = a_{1u} + a_{2u} + e_{2u}$, of which only a_{2u} is electric-dipole allowed, and therefore the transition is polarized parallel to the sixfold rotation axis (C_6). Hence, the effects shown in Fig. 3 can be understood if VBz_2 is initially formed in an essentially random orientation and then reorients upon annealing so that C_6 is normal to the surface (i.e., with the Bz rings lying flat). The 2.6 eV transition shows the opposite annealing dependence and is therefore polarized perpendicular to C_6 so that it loses intensity when the Bz rings lie flat. This would be consistent with the $a_{1g} \rightarrow e_{1u}$ transition. The $\pi \rightarrow \pi^*$ transition[15] should also be polarized parallel to C_6 since it is $e_{1g} \rightarrow e_{1u}$ or $e_{1u} \rightarrow e_{1g}$, and $e_{1g} \otimes e_{1u} = a_{1u} + a_{2u} + e_{2u}$. In Fig. 3 the $\pi \rightarrow \pi^*$ is weak and

broad, as in Fig. 2(d), and difficult to separate from the same transition in unreacted Bz; however, it is still clearly present after the 258 K anneal, which is consistent with the polarization assignment discussed above.

Deviations from complete polarization could indicate a degree of disorder in the molecular alignment or a contribution from impact scattering. The latter is a possibility since the scattering geometry in these experiments was off-specular (see Sec. II A). Theoretical studies[13,18] have shown that both orientations are possible for $TM(Cp)_2$ species on HOPG, depending on the TM, and that the energy difference is often small (<20 meV in some cases). However, a thermally induced reorientation such as that observed for VBz_2 has not to our knowledge been previously seen experimentally. The reason for the preferred orientation in the case of VBz_2, but not $CrBz_2$, is uncertain and will require further theoretical study. It is speculated that the effect may result from a weak interaction between the singly occupied V $3d_z^2$ HOMO, which lies parallel to C_6, and the HOPG π-band.

Temperature-programmed desorption (TPD) data show desorption of $CrBz_2$ from a Ni(100) surface[17] and from a CH_3-terminated n-alkanethiol self-assembled monolayer[48] (SAM) at about 250 and 265 K, respectively, and the $CrBz_2$-related structure in Fig. 2(c) disappears at about this temperature. Other TPD peaks are seen at ~300–310 K for recombinative desorption[17] of $CrBz_1$ and adsorbed Bz or from $CrBz_2$ that has penetrated into the SAM.[48] These processes do not apply in the present case since any Bz released by $CrBz_2$ dissociation would desorb from HOPG at well below 300 K,[31] and penetration of $CrBz_2$ into the HOPG lattice is unlikely. Similarly, TPD data[49] for VBz_2 show desorption at ~230 K from SiO_2 and at ~260 K from an organic SAM. For both $CrBz_2$ and VBz_2, all features in ELS or UPS vanish at room temperature, leaving only bare HOPG and a small coverage of unreacted metal that can be seen in AES. The unreacted metal residue was observed even in cases where there was initially a large excess of Bz, i.e., a thick Bz ice layer and a sub-ML equivalent of deposited Cr or V. Apparently, the TM-arene reaction is driven largely by the thermal energy of the incident TM atom since annealing up to the desorption temperature of Bz (~150 K) does not consume the unreacted TM. Likewise, a reverse process in which Bz was deposited on top of a submonolayer of TM at 100 K gave no evidence of reaction up to the Bz desorption temperature. Theory[4–6] indicates that sandwich structures of the form graphene-TM-Bz are very stable; hence, there appears to be a kinetic barrier to the formation of similar structures on HOPG below 150 K.

B. Ultraviolet photoemission spectroscopy

Figure 4(a) shows UPS data for clean HOPG that agrees with previous HeII results;[14,50] although, the major peak at ~8 eV is not as sharp, which may be due to the roughness of the present surface.[50] Figure 4(b) shows data for a layer of Bz ice, which agree with previous results[17] except that the BEs relative to the Fermi level (E_F) are ~1.5 eV higher on Ni(100) than on HOPG. This represents the combined

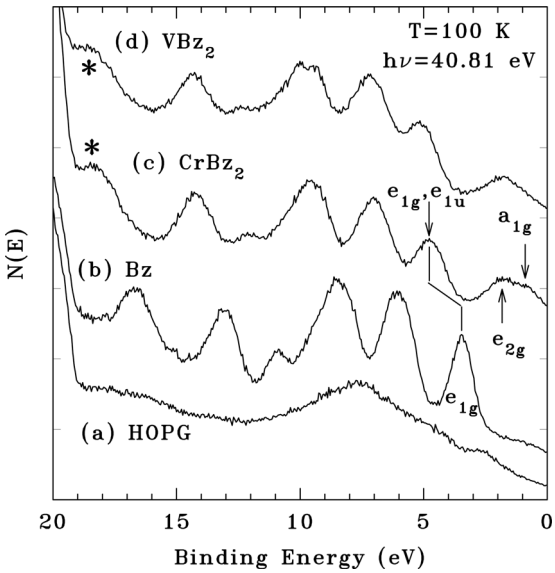

FIG. 4. UPS data (a) for bare HOPG, (b) after condensation of a layer of Bz ice, (c) after deposition of ~0.16 ML of Cr on top of Bz ice, and (d) after deposition of ~0.25 ML of V on Bz ice. All data are for HeII excitation ($h\nu = 40.81$ eV) at a sample temperature of 100 K, and binding energies are referenced to the Fermi level. The spectra have been displaced vertically for clarity. Nonzero emission above the HOMO in (b) is due to higher-energy satellites in the HeII spectrum. The off-scale emission at the high-BE end is due to excitation by the main HeI line at $h\nu = 21.22$ eV. The features marked with an asterisk in (c) and (d) may be due in part to excitation of the HOMO by the HeI satellite at $h\nu = 23.09$ eV (see text). The lines connecting (b) and (c) illustrate the correlation between features in the Bz multilayer and the $CrBz_2$ monolayer.

effects[51] of differences in the work function of the two substrates (with a Bz overlayer) and in relaxation (molecular polarization plus image-charge screening).

The UPS data for $CrBz_2$ formed *in situ* [Fig. 4(c)] agree well with those for a multilayer[17] grown by vapor deposition on Ni(100), although in the latter case, the a_{1g} and e_{2g} features are better resolved and the BEs about 0.5 eV higher. The $CrBz_2$ BEs are found, here and in Ref. 17, to increase slightly with coverage, and therefore the UPS features are less well resolved until the layer is sufficiently thick to obscure the interface. Since the amount of Cr deposited in obtaining the data in Fig. 4(c) was equivalent to only ~0.16 ML, the data represent at most a single close-packed $CrBz_2$ layer (see the supplementary material[27]). The shift to lower BE with decreasing thickness arises from an increased relaxation shift of the photoionized molecule when in direct contact with the substrate.[51] Features marked with an asterisk in Fig. 4 may be "ghosts" due to excitation of the HOMO by the 23.09 eV HeI satellite; however, they also correspond to theoretically predicted $CrBz_2$ and VBz_2 features (see below). For $CrBz_2$ on Ni(100), secondary electrons damage the adsorbate during UPS data collection.[17] For HOPG, repeated scans of the same area of the surface showed that such effects are negligible, which suggests that HOPG is a less efficient secondary-electron emitter than Ni under HeI and HeII irradiation.

There are, to our knowledge, no previous UPS data for either gas-phase or condensed VBz_2 except for a tabulation[52] of the gas-phase BEs, which shows the HOMO, HOMO-1,

and HOMO-2 all falling within a range of 0.75 eV. The data in Fig. 4(d) are very similar in all respects to those for $CrBz_2$ except for the slightly higher BE for the e_{1g},e_{1u} peak and the absence of any clear a_{1g} feature. There is also a small splitting of the peak at ~10 eV BE, which is reproducible and which vanishes after annealing at ~260 K. The temperature dependence suggests that the splitting may be related in some way to the molecular reorientation discussed above.

Figure 5 shows data for a thin layer of Tol ice and for the same layer after depositing ~0.10 ML of Cr. The Cr coverage was reduced, relative to the $CrBz_2$ experiments, in consideration of the larger "footprint" of flat-lying Tol versus Bz. There are, to our knowledge, no published UPS data for toluene ice; however, the results can be discussed with reference to HeI-excited gas-phase spectra.[53] The main difference between Bz [Fig. 4(b)] and Tol [Fig. 5(a)] ices is in the region of BE = 8–9 eV, which in Bz is assigned to the σ-bonding $3e_{1u}$ and $1b_{2u}$ orbitals. In Tol, these orbitals are perturbed by the CH_3 group, and the asymmetrically broadened Bz peak is seen to split in the Tol data. This effect, which is clearly seen in a comparison of gas-phase UPS data[54] for $CrBz_2$ and $Cr(Tol)_2$, appears in Fig. 5(b) as a distinct broadening in comparison to the corresponding $CrBz_2$ feature. This is taken to indicate that the bonding of the CH_3 to the Bz ring remains intact since no similar broadening is seen for $CrBz_2$ at any coverage.

To our knowledge, $Cr(Tol)_2$ is not commercially available; hence, Fig. 5(b) illustrates the use of *in situ* synthesis as a simple method for obtaining spectra for new molecular species. Compared to $CrBz_2$, the HOMO and HOMO-1 are broadened, even for a $Cr(Tol)_2$ multilayer (not shown). This could result from an unresolved splitting of the e_{2g} level due to the symmetry-lowering effect of the CH_3 group. Theory finds[55] that the lowest-energy configuration places the two CH_3 groups 180° apart but that there is only a small (4.5 kJ/mol or less) barrier for the relative rotation of the two rings. Hence, rotational disorder is expected in the $Cr(Tol)_2$ layer, which could contribute to broadening. In ELS data (not shown), a transition is found at 4.0 eV that is also broadened relative to that for $CrBz_2$.

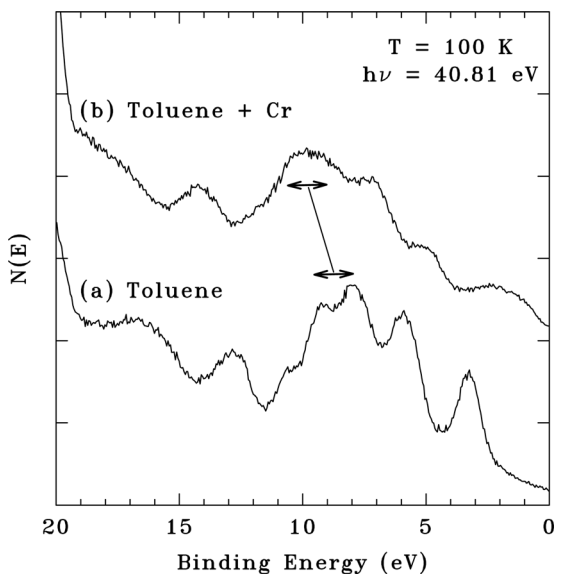

FIG. 5. (a) UPS data for a thin film (approximately one close-packed layer) of toluene on HOPG. (b) After deposition of ~0.10 ML of Cr at 100 K to form $Cr(Tol)_2$. The arrows and the connecting line identify features discussed in the text.

C. Search for doping effects

Doping via adsorption of $CrBz_2$ involves formation of the cation, $[CrBz_2]^+$. As noted in the Introduction, an analogous process was observed[14] for $CoCp_2$ and ascribed to the low IP of the free molecule. Electron transfer to the substrate was indicated by the decrease in the sample work function (ϕ_S), due to the formation of a dipole layer with the positive end above the surface, and by the emptying of the singly occupied HOMO. Furthermore, a sub-ML of $CoCp_2$ remains adsorbed on HOPG at room temperature,[14] unlike in the case of $CrBz_2$ and VBz_2, which suggests a strong bond that is consistent with electron transfer. $CoCp_2$ has also been incorporated[56] into organic electronic materials as an *n*-type dopant.

The experimental (i.e., vertical) ionization potentials (VIPs) of gas-phase $CrBz_2$ (5.40 eV, Ref. 16), VBz_2 (5.95 eV, Ref. 52; 5.78 eV, Ref. 57), and $CoCp_2$ (5.55 eV, Ref. 58) are all similar. As a test of the computational methods used here, values of 5.40 and 5.32 eV were found for the VIPs of $CrBz_2$ and $CoCp_2$ which are in reasonable agreement with experiment. In electron doping, which forms a stable cation, the adiabatic IP (AIP) is more relevant than the VIP, and calculations performed here give AIPs of 5.44, 5.62 and 5.23 eV, respectively, for gas-phase $CrBz_2$, VBz_2 and $CoCp_2$. Here, the difference in zero-point vibrational energies between the neutral and the ionized species has been included. In agreement with previous DFT results,[59] the lowest-energy configuration of the 16-electron $[VBz_2]^+$ cation is found to be a Jahn-Teller-distorted open-shell triplet rather than a closed-shell singlet. In the adsorbed state, the IPs will be reduced by ~1–1.5 eV due to screening and relaxation effects.[51] Thus, if the AIP is the controlling factor, then electron transfer to HOPG should occur as readily for $CrBz_2$ as for $CoCp_2$, which was a motivating factor in the present experiments. It should be noted, however, that recent theoretical work[13] suggests that it is the overlap of the bis(arene)TM HOMO with the graphene π orbitals, and not simply the AIP, that is critical in electron transfer.

Figure 6 shows UPS data for $CrBz_2$ at 100 K together with DFT results for the neutral and cationic species. The $CrBz_2$ coverage in Fig. 6(a) is somewhat higher than in Fig. 4(c), and the spectrum shows the sharper structure and slightly higher BEs associated[17] with a multilayer. The $[CrBz_2]^+$ calculation was spin-unrestricted, and the results shown are for the total spin-up plus spin-down spectrum. Geometry optimization for $[CrBz_2]^+$ showed that the eclipsed structure is favored over the staggered by 3.1 kJ/mol. For the neutral molecule the computed energy difference is 4.1 kJ/mol, in good agreement with previous results.[36] The relative intensities and BEs computed for VBz_2 (not shown), which is isoelectronic with $[CrBz_2]^+$, are very similar to those in Fig. 6(c). Likewise, the computed UPS of $[VBz_2]^-$ (not shown) is similar to that of $CrBz_2$.

Upon (computational) formation of $[CrBz_2]^+$ the now-singly occupied HOMO shifts higher in BE, to the point where it cannot easily be distinguished from the HOMO-1, and the HOMO-1 and HOMO-2 shift by about 0.7 and 0.4 eV, respectively, to higher BE. The computed BE shifts are assumed to be reliable, even though the absolute BEs are somewhat overestimated due to the difficulty in accurately describing strongly correlated TM 3d electrons[60] in conventional DFT. This strong correlation accounts for the fact that all orbitals with a significant Cr 3d component shift in BE when a single electron is removed from the HOMO. In the experimental $CrBz_2$ spectrum [both Figs. 4(c) and 6(a)] the a_{1g} HOMO is clearly visible, with an a_{1g}/e_{2g} relative intensity similar to that in the computed $CrBz_2$ spectrum. The appearance of the experimental HOMO and HOMO-1 is unlike that in the computed $[CrBz_2]^+$ or experimental VBz_2 spectra, which argues against cation formation. Another strong argument against cation formation is that the appearance of the HOMO and HOMO-1 (i.e., relative intensity and BE versus the Bz ring orbitals) is essentially the same, aside from additional broadening, for a thin layer in which the $CrBz_2$ is in close proximity to the surface as it is for a multilayer or for the free molecule (Fig. 1).

Hole doping is considered unlikely for the present systems. A calculation for the $[CrBz_2]^-$ anion (not shown) resulted in a singly occupied HOMO centered at 2.8 eV above the e_{2g} level (i.e., at E_F), which has no counterpart in the data. The adiabatic electron affinity (AEA) of gas-phase $CrBz_2$, found computationally[61] to be −0.14 eV, indicates that the anion is unstable relative to the neutral species, although screening and/or image-charge effects could lower the energy of an adsorbed anion. In any case, the AEA is much less than φ_S of bare HOPG (4.6 eV), which prohibits electron transfer from HOPG. VBz_2 is a 17-electron system; hence, one might expect that electron transfer from HOPG, to form $[VBz_2]^-$, might be energetically favorable. However, theory[61] and experiment[62] show that the free anion is unstable against ejection of an electron, although $[VBz_2]^-$ has been prepared in solution[63] through contact with K metal. A further discussion of this breakdown of the 18-electron rule, which is based on a simple one-electron description of the bis(arene)TM orbital structure, is beyond the scope of the present work.

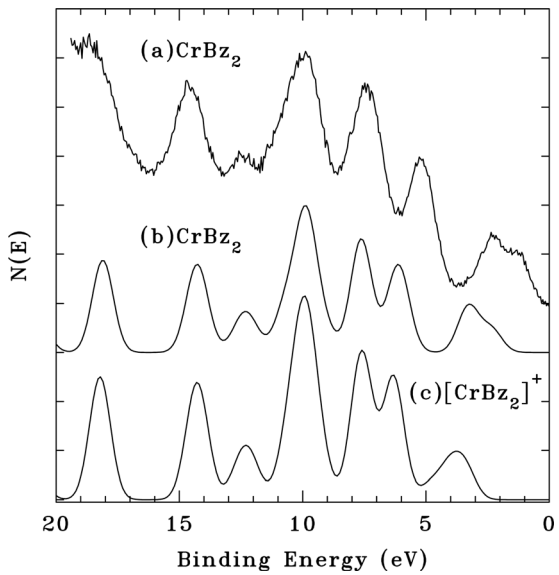

FIG. 6. (a) UPS for $CrBz_2$ (100 K, $h\nu = 40.81$ eV). (b) Computed DOS for the free $CrBz_2$ molecule. (c) Same as (b) but for the molecular cation. Both calculated spectra have been shifted in energy to bring the peak at 10.0 eV into approximate alignment with the experimental spectrum. This obscures any shift between the neutral and the cationic molecules and was done in order to make clear the relative shifts in the HOMO and HOMO-1. Note that $[CrBz_2]^+$ and VBz_2 are isoelectronic.

In this work, any effect on φ_S resulting from electron transfer to or from $CrBz_2$ or VBz_2 is difficult to detect due to the presence of small amounts of unreacted metal, which have a large effect on φ_S. Theoretical work[64] for Cr on graphene finds a charge of $+0.58\,e$ on an isolated Cr atom which, for a C–Cr distance of 1.95 Å (the sum of covalent radii), yields a dipole moment of 5.43 Debyes. For the adsorption of n dipoles/cm^2 with a surface-normal moment of $\mu_\perp$ Debyes, $\delta\varphi_S(\text{eV}) = 3.00 \times 10^{-16} \cdot (4\pi n \mu_\perp)$ gives the change in φ_S. Thus, $\delta\varphi_S \approx -1.0$ eV (a typical result for *in situ* $CrBz_2$ formation) corresponds to $n \approx 4.9 \times 10^{13}$ Cr/cm^2, or ~0.013 ML (~5–10% of the total Cr in a typical experiment). This is only a rough estimate since it is based on $\delta\varphi_S$ for a continuous layer of dipoles; however, it demonstrates the sensitivity of $\delta\varphi_S$ to adsorbed TM atoms. The decrease in φ_S, due to the surface dipole layer formed by the unreacted TM, will shift all the $TM(Bz)_2$ orbitals (which shift together with the vacuum level) to correspondingly higher BE relative to E_F, which will then impede electron transfer to the HOPG. Adsorption of $CoCp_2$ on HOPG also results in a large decrease[14] in φ_S ($\delta\varphi_S = -1.2$ eV), but in this case it is due to the electron transfer itself rather than to a foreign species acting independently. Upon warming, $\delta\varphi_S$ decreases somewhat in magnitude, presumably due to the clustering[22,23] of unreacted TM atoms.

IV. CONCLUSIONS

In summary, thin bis(arene)TM layers on HOPG have been formed *in situ* in an UHV chamber by depositing the metal on top of a film of arene ice at 100 K. The valence electronic structure of the molecular species was then examined using ELS and UPS. The results are as follows:

1. Depositing a TM on a condensed layer of a simple arene[20] appears to be a general method for *in situ* formation of a bis(arene)TM. The process is "clean" in that there is no indication of side reactions or unwanted by-products, although the presence of a small coverage of unreacted TM atoms appears unavoidable. A simple ring substituent (CH_3) remains intact during the reaction. Thus, it should be possible to synthesize and study species that are not readily available (or cannot easily be made) in bulk form or that have too low a vapor pressure to allow easy *in situ* deposition.
2. Data have been obtained for VBz_2 and $Cr(Tol)_2$, the valence structures of which have not previously been studied in detail using UPS and ELS. Although deeper-lying arene orbitals are essentially unperturbed by formation of the bis(arene)TM sandwich, subtle differences in the HOMO and HOMO-1 have been observed and discussed

in comparison to $CrBz_2$ with the aid of DFT modeling. In the case of VBz_2, clear evidence is seen for a molecular reorientation during annealing, based on the ELS polarization dependence.

3. Charge transfer between an adsorbed bis(arene)TM and HOPG depends on the occupancy of the molecular HOMO and on its energy relative to E_F. The small amount of unreacted TM that results from *in situ* synthesis causes a large decrease in work function, which shifts the adsorbate HOMO to below E_F and thus impedes electron transfer to the HOPG. This is an obstacle to forming doping layers by this method.

ACKNOWLEDGMENTS

This work was supported by the Office of Naval Research and by a grant of computer time from the DOD High Performance Computing Modernization Program at the ARL-MSRC. J. P. Long is thanked for providing the UPS excitation source, and H. Pinto is thanked for helpful communications. D. E. Barlow and A. R. Laracuente are thanked for helpful discussions.

[1]L. Duclaux, Carbon **40**, 1751 (2002).
[2]J. Zhao and R.-H. Xie, J. Nanosci. Nanotechnol. **3**, 459 (2003).
[3]M. Terrones, A. G. Souza Filho, and A. M. Rao, *Carbon Nanotubes: Advanced Topics in Synthesis, Structure, Properties and Applications*, Topics in Applied Physics, Vol. 111, edited by A. Jorio, G. Dresselhaus, and M. S. Dresselhaus (Springer, Berlin, 2008), p. 531.
[4]P. Plachinda, D. R. Evans, and R. Solanki, J. Chem. Phys. **135**, 044103 (2011).
[5]S. M. Avdoshenko, I. N. Ioffe, G. Cuniberti, L. Dunsch, and A. A. Popov, ACS Nano **5**, 9939 (2011).
[6]H. Pinto, R. Jones, J. P. Goss, and P. R. Briddon, Phys. Rev. B **82**, 125407 (2010). In this reference, the text states that in the graphene-Cr-toluene sandwich the Cr is η^1 with respect to the graphene (i.e., directly above a C atom); whereas, it is shown as η^6 in the accompanying figure (Fig. 10). The latter configuration is correct (H. Pinto, personal communication, 7 September 2011).
[7]E. L. Muetterties, J. R. Bleeke, E. J. Wucherer, and T. A. Albright, Chem. Rev. **82**, 499 (1982).
[8]H. Shiozawa, C. E. Giusca, S. R. P. Silva, H. Kataura, and T. Pichler, Phys. Status Solidi B **245**, 1983 (2008).
[9]W. Plank, H. Kuzmany, R. Pfeiffer, T. Saito, and S. Iijima, Phys. Status Solidi B **246**, 2724 (2009).
[10]A. Chernov *et al.*, Phys. Status Solidi B **249**, 2323 (2012).
[11]J. Lu, S. Nagase, D. Yu, H. Ye, R. Han, Z. Gao, S. Zhang, and L. Peng, Phys. Rev. Lett. **93**, 116804 (2004).
[12]E. L. Sceats and J. C. Green, Phys. Rev. B **75**, 245441 (2007).
[13]Y. Li, X. Chen, G. Zhou, W. Duan, Y. Kim, M. Kim, and J. Ihm, Phys. Rev. B **83**, 195443 (2011).
[14]O. Henrion and W. Jaegermann, Surf. Sci. **387**, L1073 (1997).
[15]V. M. Rayón and G. Frenking, Organometallics **22**, 3304 (2003).
[16]J. G. Brennan, G. Cooper, J. C. Green, N. Kaltsoyannis, M. A. MacDonald, M. P. Payne, C. M. Redfern, and K. H. Sze, Chem. Phys. **164**, 271 (1992).
[17]P. M. Blass, S. Akhter, C. M. Seymour, J. J. Lagowski, and J. M. White, Surf. Sci. **217**, 85 (1989).
[18]H. S. Kang and A. Pramanik, J. Chem. Phys. **135**, 124708 (2011).
[19]J. T. S. Andrews, E. F. Westrum, Jr., and N. Bjerrum, J. Organomet. Chem. **17**, 293 (1969).
[20]W. Sklarek, G. Held, C. Ammon, and H.-P. Steinrück, Appl. Surf. Sci. **142**, 327 (1999).
[21]F. G. N. Cloke and P. L. Arnold, *Comprehensive Organometallic Synthesis III*, edited by R. H. Crabtree and D. M. P. Mingos (Elsevier, Amsterdam, 2007), Vol. 1, p. 219.
[22]C. Binns, S. H. Baker, C. Demangeat, and J. C. Parlebas, Surf. Sci. Rep. **34**, 107 (1999).
[23]V. D. Borman, M. A. Pushkin, V. N. Tronin, and V. I. Troyan, Zh. Eksp. Teor. Fiz. **137**, 1151 (2010) [J. Exp. Theor. Phys. **110**, 1005 (2010)].
[24]P. Oelhafen and J. L. Freeouf, J. Vac. Sci. Technol. A **1**, 96 (1983).
[25]A. Güttler, Th. Zecho, and J. Küppers, Chem. Phys. Lett. **395**, 171 (2004).
[26]J. J. McClelland, J. Unguris, R. E. Scholten, and D. T. Pierce, J. Vac. Sci. Technol. A **11**, 2863 (1993).
[27]See supplementary material at http://dx.doi.org/10.1116/1.4794194 for a description of how Cr and V coverages were determined using AES.
[28]M. D. Healy, D. C. Smith, R. R. Rubiano, N. E. Elliott, and R. W. Springer, Chem. Mater. **6**, 448 (1994).
[29]K. D. Childs, B. A. Carlson, L. A. LaVanier, J. F. Moulder, D. F. Paul, W. F. Stickle, and D. G. Watson, *Handbook of Auger Electron Spectroscopy*, edited by C. L. Hedberg (Physical Electronics, Eden Prairie, MN, 1995).
[30]C. T. Campbell and S. M. Valone, J. Vac. Sci. Technol. A **3**, 408 (1985).
[31]R. Zacharia, H. Ulbricht, and T. Hertel, Phys. Rev. B **69**, 155406 (2004).
[32]M. D. Antonik, R. J. Lad, and T. M. Christensen, Surf. Interface Anal. **24**, 681 (1996).
[33]M. J. Frisch *et al.*, *Gaussian 09*, Revs. A01, B01, and C01 (Gaussian, Wallingford, CT, 2009).
[34]F. Furche and J. P. Perdew, J. Chem. Phys. **124**, 044103 (2006).
[35]M. Dolg, U. Wedig, H. Stoll, and H. Preuss, J. Chem. Phys. **86**, 866 (1987).
[36]A. Perrier, D. Gourier, L. Joubert, and C. Adamo, Phys. Chem. Chem. Phys. **5**, 1337 (2003).
[37]H. B. Schlegel and J. J. W. McDouall, *Computational Advances in Organic Chemistry: Molecular Structure and Reactivity*, edited by C. Ögretir and I. G. Csizmadia (Kluwer, Dordrecht, 1991), p. 167.
[38]L. Calliari, S. Fanchenko, and M. Filippi, Surf. Interface Anal. **40**, 814 (2008).
[39]O. Kröhl and P. Swiderek, J. Mol. Struct. **480–481**, 237 (1999).
[40]M. Shiho, J. Phys. Soc. Jpn. **43**, 2105 (1977).
[41]M. C. Schalnat, A. M. Hawkridge, and J. E. Pemberton, J. Phys. Chem. C **115**, 13717 (2011).
[42]C. E. Moore, *Atomic Energy Levels* (US Government Printing Office, Washington, DC, 1949), Vol. II, National Bureau of Standards Circular 467.
[43]S. Yu. Ketkov, G. A. Domrachev, and G. A. Razuvaev, J. Mol. Struct. **195**, 175 (1989).
[44]J. I. Martínez, J. M. García-Lastra, M. J. López, and J. A. Alonso, J. Chem. Phys. **132**, 044314 (2010).
[45]M. P. Andrews, S. M. Mattar, and G. A. Ozin, J. Phys. Chem. **90**, 1037 (1986).
[46]G. W. Rubloff, Solid State Commun. **26**, 523 (1978).
[47]A. Borghesi and G. Guizzetti, *Handbook of Optical Constants II*, edited by E. D. Palik (Academic, Orlando, FL, 1991), p. 449.
[48]S. Nagaoka, K. Ikemoto, T. Matsumoto, M. Mitsui, and A. Nakajima, J. Phys. Chem. C **112**, 6891 (2008).
[49]T. Matsumoto, S. Nagaoka, K. Ikemoto, M. Mitsui, M. Ara, H. Tada, and A. Nakajima, Eur. Phys. J. D **52**, 99 (2009).
[50]A. Mansour and P. Oelhafen, Appl. Phys. A **58**, 437 (1994).
[51]J. E. Demuth and D. E. Eastman, Phys. Rev. Lett. **32**, 1123 (1974).
[52]F. G. N. Cloke, A. N. Dix, J. C. Green, R. N. Perutz, and E. A. Seddon, Organometallics **2**, 1150 (1983).
[53]K. Kimura, S. Katsumata, Y. Achiba, T. Yamazaki, and S. Iwata, *Handbook of HeI Photoelectron Spectra of Fundamental Organic Molecules* (Halsted, New York, 1981).
[54]S. Evans, J. C. Green, and S. E. Jackson, J. Chem. Soc., Faraday Trans. 2 **68**, 249 (1972).
[55]I. P. Gloriozov, A. Yu. Vasil'kov, and Yu. A. Ustynyuk, Zh. Fiz. Khim. **80**, 476 (2006) [Russ. J. Phys. Chem. **80**, 394 (2006)].
[56]C. K. Chan, F. Amy, Q. Zhang, S. Barlow, S. Marder, and A. Kahn, Chem. Phys. Lett. **431**, 67 (2006).
[57]B. R. Sohnlein, Y. Lei, and D.-S. Yang, J. Chem. Phys. **127**, 114302 (2007).
[58]J. Brennan, G. Cooper, J. C. Green, M. P. Payne, and C. M. Redfern, J. Electron Spectrosc. Relat. Phenom. **66**, 101 (1993).
[59]T. D. Jaeger, D. van Heijnsbergen, S. J. Klippenstein, G. von Helden, G. Meijer, and M. A. Duncan, J. Am. Chem. Soc. **126**, 10981 (2004).
[60]N. J. Mosey and E. A. Carter, Phys. Rev. B **76**, 155123 (2007).
[61]H. Li, C. Li, H. Fan, and J. Yang, J. Mol. Struct.: THEOCHEM **952**, 67 (2010).
[62]K. Judai, M. Hirano, H. Kawamata, S. Yabushita, A. Nakajima, and K. Kaya, Chem. Phys. Lett. **270**, 23 (1997).
[63]Ch. Eischenbroich and F. Gerson, J. Am. Chem. Soc. **97**, 3556 (1975).
[64]H. Valencia, A. Gil, and G. Frapper, J. Phys. Chem. C **114**, 14141 (2010).